

Vortex relaxation and coupling in superconducting heterostructures studied by STM

G.J.C. van Baarle, F. Galli, P. H. Kes and J. Aarts
*Kamerlingh Onnes Laboratory, Leiden University,
 P.O. Box 9504, 2300 RA Leiden, The Netherlands*
 (Dated: September 28, 2017)

In a sandwich consisting of two superconducting films, one weakly pinning and one strongly pinning, the vortex positions in both films are determined by the strongly pinning material and the vortex lattice is disordered in both films. We used (strongly pinning) NbN and (weakly pinning) $a\text{-Mo}_{2.7}\text{Ge}$ and studied, by directly imaging the vortex core positions with a scanning tunnelling microscope, how this disorder is restored with increasing thickness of $a\text{-Mo}_{2.7}\text{Ge}$ layer or when the interface is made insulating. For clean interfaces we find that the first reordering of the vortex lattice is found at a layer thickness which is compatible with the first bending mode of the vortex lines. Making the interface insulating we find that order is restored quickly. We argue that this is can be understood from the competition between the Josephson force working on the vortex segments on the one hand, and the elastic restoring forces inside the weakly pinning layer on the other hand.

PACS numbers: 74.25.Qt,74.50.+r

I. INTRODUCTION

In the investigation of the properties of vortices and vortex lattices in type-II superconductors, direct imaging of the vortex positions at the surface of the material can be a useful tool. For magnetic fields of practical interest the distance between vortex lines becomes small (roughly 50 nm at 1 T) and Scanning Tunnelling Microscopy (STM) gains an advantage over magnetic imaging techniques since STM is only sensitive to the vortex cores. A disadvantage of the technique is that the sample surface needs to be clean and conducting. For crystals, this can be done by breaking or cleaving, which has been successful for such materials as NbSe_2 [1, 2] or $\text{Bi}_2\text{Ca}_2\text{SrCu}_2\text{O}_{8-\delta}$ [3, 4]. For thin films no such simple preparation method exists and since surfaces easily oxidize, reports on vortex imaging on superconducting films are relatively few. One way to overcome this problem is to protect the film surface with a thin capping layer of a noble metal such as Au. As we showed before, this works well on films of $a\text{-Mo}_{2.7}\text{Ge}$, a weakly pinning superconductor, capped with 3 nm Au and clear images of the vortex structure could be obtained by mapping the proximity-induced gap at the Au surface [5]. The Au layer should be flat, which means that Au should be wetting the surface during deposition, and the interface should be transparent. Neither condition is always met. For instance, although a reasonably flat Au film forms on films of strongly pinning NbN, spectroscopy shows very unclear vortex images, presumably because the rough NbN surface causes a bad NbN / Au interface. This can be overcome by depositing a thin (20 nm) film of $a\text{-Mo}_{2.7}\text{Ge}$ followed by the Au protection layer. Clear vortex contrast could again be obtained, and showed the NbN vortex lattice (VL) to be completely disordered [5]. This use of a $a\text{-Mo}_{2.7}\text{Ge}/\text{Au}$ template layer assumes that the vortex positions as fixed by the NbN layer are transferred in true fashion to the Au surface, which should be the case when the $a\text{-Mo}_{2.7}\text{Ge}$ layer is too thin to yield ap-

preciable bending or rearrangement of the vortex cores. In this work we further address this issue, which consists of two parts. The first involves the vortex-vortex interactions within the template layer, which might lead to reorientation of the vortices in that layer or, more specifically, to the recurrence of the well-ordered $a\text{-Mo}_{2.7}\text{Ge}$ VL. The second question is with respect to the coupling of the vortices in the two superconducting layers. If the interface has a metallic character, the proximity effect will play a major role in coupling the vortices; if the surface of the host superconductor is insulating, as is often the case in oxide materials, the coupling may become of the Josephson type, or merely electromagnetic, and this can allow freedom for the vortex in the template to move with respect to the one in the host.

The structure of the paper is as follows. We first introduce the experimental techniques and the data analysis process, in particular the use of the autocorrelation function. Then we address the question of the length scale on which the disorder injected by the NbN layer is healed in the $a\text{-Mo}_{2.7}\text{Ge}$ template layer, by measuring samples with different (template) thicknesses d_t of the $a\text{-Mo}_{2.7}\text{Ge}$ -layer. We show data on the variation of the autocorrelation functions as function of d_t , and we discuss them by considering the bending modes of vortex lines in $a\text{-Mo}_{2.7}\text{Ge}$. Then we present experimental results on the issue of coupling, by studying heterostructure samples with a badly conducting or insulating interface layer. In the discussion, we consider the strength of the electromagnetic and Josephson coupling forces which couple the vortex segments in the two superconducting layers. This coupling is in competition with the inter-vortex forces within the template layer, which tend to reorient the vortices to their triangular arrangement.

II. EXPERIMENTAL DETAILS AND DATA PROCESSING

In this work $a\text{-Mo}_{2.7}\text{Ge}$ is used as a template layer because of its suitable properties. With a Ginzburg-Landau parameter $\kappa \approx 100$ it is a strong type-II superconductor, while its amorphous structure makes it a relatively weakly pinning material. Furthermore, its large London penetration depth λ_L yields a small tilt modulus c_{44} , which means that the VL retains a two-dimensional (2D) character up to quite large thicknesses, as will be discussed below. Finally, amorphous materials show very flat surface characteristics. The $a\text{-Mo}_{2.7}\text{Ge}$ layers were rf-sputtered from a composite Mo/Ge target in Ar atmosphere. The film thickness ranged from 25 nm to 100 nm. When necessary, we denote the thickness by $a\text{-Mo}_{2.7}\text{Ge}(x)$, with x the thickness in nm. During sputtering the substrate was water-cooled and after each minute of sputtering, and interruption of 1 minute was made to prevent heating and possible recrystallization of the films. The sputtering rate was chosen as ~ 8 nm/minute. The superconducting transition temperature T_c was 5.7 K for the 25 nm films, increasing up to 6.3 K for $d_t = 50$ nm, after which T_c became constant. The critical current for onset of vortex motion for a 500 nm thick film was found to be or the order of 10^6 A/m². Also relevant is the value of the critical field B_{c2} at the measurement temperature of 4.2 K, which was about 4.2 T for $d_t = 25$ nm, increasing to 5.2 T for $d_t = 50$ nm and beyond. The STM measurements were performed in fields up to 1 T, which means maximum reduced fields $b = B/B_{c2} \approx 0.2 - 0.3$. The strongly pinning NbN films ($J_c > 10^8$ A/m²) were reactively rf-sputtered from a Nb target in an Ar/N₂ atmosphere on Si substrates. Throughout the study, we used a thickness of 67 nm. The films are polycrystalline, as is known from high resolution transmission electron microscopy studies [6]. The rms-roughness of the films was determined by AFM to be 1.5 nm, measured on a fresh NbN surface area of $1 \times 1 \mu\text{m}$. The films showed a T_c of 11.4 K and a superconducting coherence length $\xi = 4.7$ nm.

Protective Au films were rf-sputtered in two steps. First, about 2 nm was sputtered in a pure Ar atmosphere; next, oxygen (partial pressure 5 %) was mixed in the sputtering gas, and another layer of 2 nm was sputtered. This O₂-addition promotes the formation of smaller Au grains which improves the resolution of the measurements.

The STM-setup was the same as in a previous report [2], with the sample immersed in liquid He after it was mounted in air. In this procedure field-cooled measurements are not possible, since the level of the liquid is higher than the magnet. All data were therefore taken by zero-field-cooling the sample, and then increasing the magnetic field. For all experiments we employed full current(I)-voltage(V) spectroscopy, with a single curve consisting of 200-300 points. The voltage range was chosen such that a good fit could be made to the Ohmic resistance outside the gap region, in practise typically ± 4 mV.

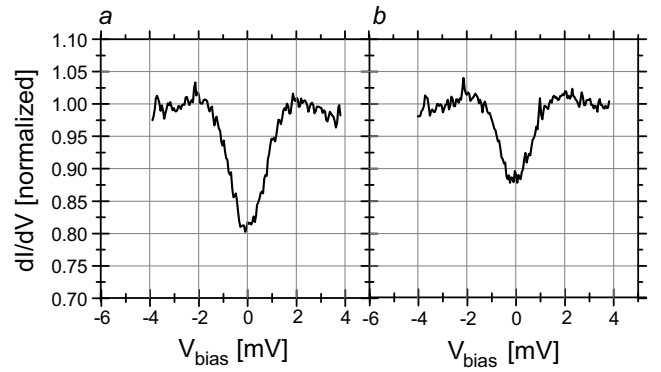


FIG. 1: Averaged normalized derivatives dI/dV for two samples, acquired at $T = 4.2$ K and $B = 0.3$ T. (a) Sample NbN/MoGe(50)/Au(6); (b) Sample NbN/MoGe(50)/Au(10)

Several curves were taken per pixel, and images typically contained 128×128 pixels. The total acquisition time for such an image was of the order of 30 minutes to 1 hour, depending on the surface quality. The maximum scan size, for the given grid, is determined by the vortex core size. The vortex signature is visible in a region with a diameter of roughly 4ξ , and needs about 3 pixels in this region for a proper determination. This yields 7 nm per pixel, and a scan size of maximally $0.9 \mu\text{m}$. The vortex positions were found by taking the ratio of the zero-bias and high-bias slopes, as obtained by numerical differentiation. Theoretically, this is a value between 0 (full gap) and 1 (no gap). In practise the gap is not well developed due to the finite temperature and the proximizing Au layer and in the gap regime the ratio is of the order 0.8. The resulting range (0.8 to 1) is then translated into a grey scale. Fig. 1 shows the effect of the thickness of the Au layer by comparing the gaps for two samples NbN/MoGe(50)/Au, where the first one has a Au layer thickness of 6 nm, while the Au layer of the second one is almost two times thicker.

A useful way of determining the amount of correlation of vortex positions is to compute the two-dimensional autocorrelation function $G(\mathbf{r})$ for a given image, defined as $G(\mathbf{r}) = \langle \rho(\mathbf{r}_1)\rho(\mathbf{r}_1 + \mathbf{r}) \rangle$. The function computes the overlap of the image with a copy of itself which is displaced by a vector \mathbf{r} . In the actual calculation, the result is normalised in order to correct for the decreasing amount of datapoints available with increasing r . Fig. 2 gives the result of this procedure for a VL imaged on a $a\text{-Mo}_{2.7}\text{Ge}$ -film of 48 nm thick at an applied field B of 0.8 T. Triangulation (Fig. 2b) shows that the VL is quite free of defects. The autocorrelation map of $G(\mathbf{r})$ (Fig. 2c) shows very little blurring towards the edges, and makes evident that the VL has both high translational and rotational bond order. By making a cross-section along a direction from the center of the image through one of the points of the hexagon, the loss of correlations can be quantified. (Fig. 2d) shows such a cross-section, plotted in units r/a_0

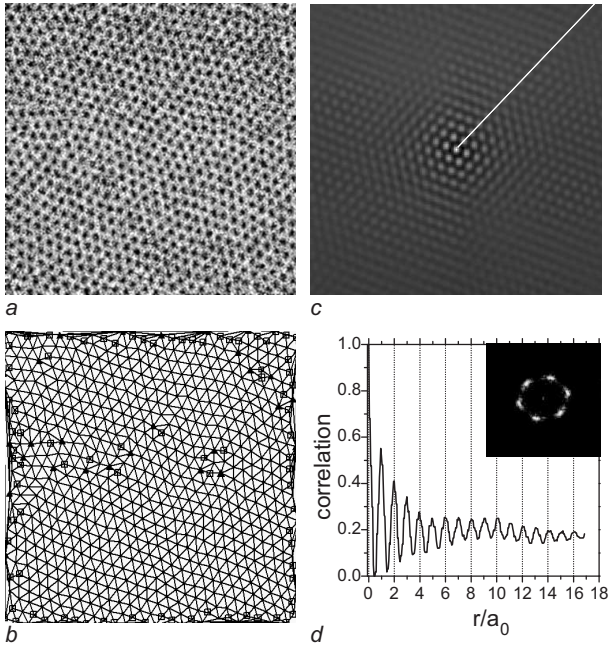


FIG. 2: (a) Vortex lattice (VL) image on a sample MoGe(48)/Au, acquired at $T = 4.2$ K and $B = 0.8$ T. The scan size is $1.2 \mu\text{m} \times 1.2 \mu\text{m}$. The raw data were smoothed with a Gaussian filter of 1 pixel width; (b) Triangulation representation of the VL. The lines represent bonds, the symbols denote deviations from the 6-fold coordination of the perfect triangular lattice (triangles (squares) : 7-fold (5-fold) coordination); (c) Normalized autocorrelation map. (d) Cross-section of the autocorrelation map along the white line in (c). The inset gives the central part of the 2D-Fourier transform of the direct-space image given in (a)

and normalized to the value at $r/a_0 = 0$. Here, a_0 the intervortex distance given by $a_0 = 1.07\sqrt{\Phi_0}/B$. It appears that r_c (somewhat arbitrarily defined as the displacement vector where the autocorrelation function does not show lattice periodicity anymore) is larger than $16 a_0$ [7].

In contrast, the VL in NbN is almost completely disordered, as shown in Fig. 3 for a 50 nm film with a Au capping layer. In this case, we find $r_c \approx 1.5a_0$ and almost no orientational correlation. Note also the relatively poor quality of the vortex image, due to the fact that no a -Mo_{2.7}Ge-template layer is present. Next we shall investigate how this disorder propagates through an intervening a -Mo_{2.7}Ge layer.

III. HEALING OF THE VORTEX LATTICE

A. Experimental data

In order to investigate on what length scale the VL disorder starts to approach the a -Mo_{2.7}Ge hexagonal lattice again, we recorded vortex images at three field values (0.2 T or 0.3 T, 0.7 T or 0.8 T, and 1 T) for NbN/ a -

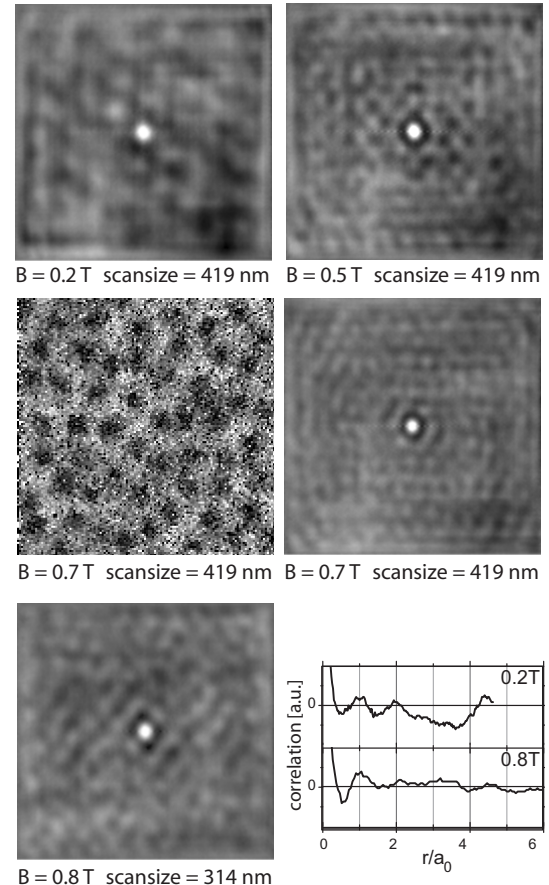


FIG. 3: Compilation of results of vortex lattice (VL) imaging of a sample NbN(50)/Au. The middle panel in the left-hand corner shows a VL image acquired at $T = 4.2$ K and $B = 0.7$ T. The adjacent panel shows the normalized autocorrelation map computed from these data. Other panels show autocorrelation map at fields of 0.2 T, 0.5 T and 0.8 T. The lower right-hand panel shows cross-sections of the autocorrelation images taken at 0.2 T and 0.8 T.

Mo_{2.7}Ge/Au samples with $d_t = 0, 25, 50$ and 100 nm. In Fig. 4 we show the autocorrelation (acr) results computed from the raw vortex images as measured in either $B = 0.7$ or $B = 0.8$ T, for the samples with $d_t = 0, 25, 100$ nm, together with one real image for $d_t = 50$ nm as a sample of the data quality. Since the contrast and the noise-level of the data are affected by the varying experimental conditions the relevance lies in the the periodicity of the structures. The gray-scale of the acr-images is chosen such that the structure of the data is clearly visible. From the data it appears that for the thinnest a -Mo_{2.7}Ge layer, the vortex positions are basically unchanged. The first ring at $r = a_0$ stands out more clearly, but that is simply due to the better data quality. There is also some increased intensity at the hexagon corners, indicating the onset of orientational order. On increasing the thickness of the a -Mo_{2.7}Ge layer we find that both the transversal and orientational order develops more and more. This is better followed in the cross-sections of the

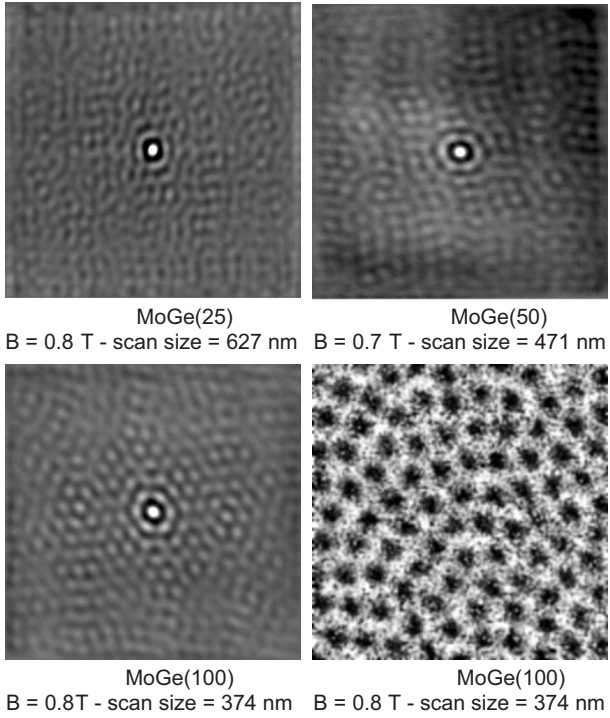


FIG. 4: Compilation of autocorrelation functions resulting from vortex lattice (VL) imaging of samples NbN(67)/*a*-Mo_{2.7}Ge(*d*_{*t*})/Au, with *d*_{*t*} = 25 nm, 50 nm, 100 nm acquired at T = 4.2 K and fields of either B = 0.7 T or 0.8 T as indicated. The lower right-hand corner shows real space data.

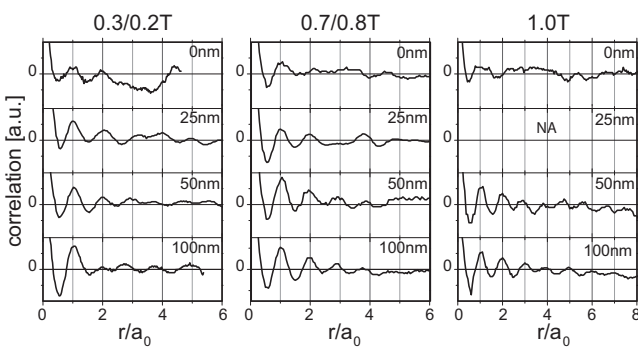


FIG. 5: Cross-sections from the autocorrelation maps of vortex lattices measured on samples NbN(67)/*a*-Mo_{2.7}Ge(*d*_{*t*})/Au, with *d*_{*t*} = 0 nm, 25 nm, 50 nm, and 100 nm acquired at T = 4.2 K and fields of either B = 0.7 T or 0.8 T as indicated.

acr-images presented in Fig. 5. Clearly, the reordering occurs but slowly. For *d*_{*t*} = 25 nm, *r*_{*c*}/*a*₀ ≈ 2 at all fields. For 100 nm, this has increased to about 4 (in the 0.8 T data) or maybe 6 (in the 1 T data). Although the signature for healing therefore is unequivocally present, the order at a *a*-Mo_{2.7}Ge thickness of 100 nm is still far less than in the unconstrained vortex lattice.

B. Bending modes in *a*-Mo_{2.7}Ge.

In order to understand this length scale, we next consider the length over which a vortex line can bend. This involves both tilting the line and shearing it with respect to the whole VL. Starting from a 2D collectively pinned VL, we can estimate the film thickness where the first bending starts to be relevant. The extent to which deformations can develop in the transverse and longitudinal direction depends on the balance of the tilt and shear energy densities *E*_{*s,t*} which are given in the elastic limit by *E*_{*s*} = $\frac{1}{2}c_{66}(u/s)^2$ for shear deformations (with *c*₆₆ the shear modulus of the VL) and *E*_{*t*} = $\frac{1}{2}c_{44}(u/l)^2$ (with *c*₄₄ the tilt modulus of the VL) for tilt deformations of a vortex in a medium where *s* and *l* respectively are the transversal and longitudinal axis of the cigar-shaped surface with constant displacement *u* (with *u* ≪ *a*₀ in order to be in the linear regime). The energy balance leads to a relation for the ratio between *s* and *l*:

$$l = s \sqrt{\frac{c_{44}(k_{\perp}, k_{\parallel})}{c_{66}}} \quad (1)$$

This means that if we set the typical length scale for longitudinal deformations to the film thickness (*l* = *d*), the typical transverse length scale *s* is set by the square root of the ratio of the elastic constants. The smallest transverse length scale is simply given by *s* = *a*₀. The thickness *d*_{max} where these deformations start to be relevant can be obtained by neglecting the very small dispersion of *c*₆₆ and taking for *c*₄₄ = *c*₄₄(*k*_⊥, *k*_{||}):

$$c_{44}(k_{\perp}, k_{\parallel}) = \frac{c_{44}(0)}{1 + \lambda^2(k_{\perp}^2 + k_{\parallel}^2)} \approx \frac{c_{44}(0)}{\lambda^2(k_{\perp}^2 + k_{\parallel}^2)}, \quad (2)$$

where *c*₄₄(0) = *B*²/*μ*₀; in the last step we made use of the fact that $\lambda \gg a_0$, as well as that $b \leq 0.3$ (making a field correction for λ unnecessary). Since λ is very large, we use the non-local expression. The wavevector *k*_⊥ for tilt deformations runs from 0 to *K*₀, the Brillouin zone boundary. In a circular approximation the Brillouin zone boundary is given by *K*₀ = (4π²*B*/*Φ*₀)^{1/2}. In principle one should integrate over all the values for *k*_⊥, but from eq. 2 we find that the large *k*-contributions dominate, leading to the approximation:

$$c_{44}(k_{\perp}, k_{\parallel}) \approx \frac{c_{44}(0)}{\lambda^2 \left(\left(\frac{2\pi}{a_0} \right)^2 + k_{\parallel}^2 \right)}. \quad (3)$$

In case of a given vortex length *d* the wavevector *k*_{||} for tilt deformations is quantized: *k*_{||} = *n*π/*d* with *n* ∈ \mathbb{N} . Since we are looking for the case that the vortex line just starts to bend, we are interested in the case where the *n* = 1 mode becomes relevant, which leads to the expression

$$c_{44}(k_{\perp}, k_{\parallel}) \approx \frac{c_{44}(0)}{\lambda^2 \left(\left(\frac{2\pi}{a_0} \right)^2 + \left(\frac{\pi}{d} \right)^2 \right)}. \quad (4)$$

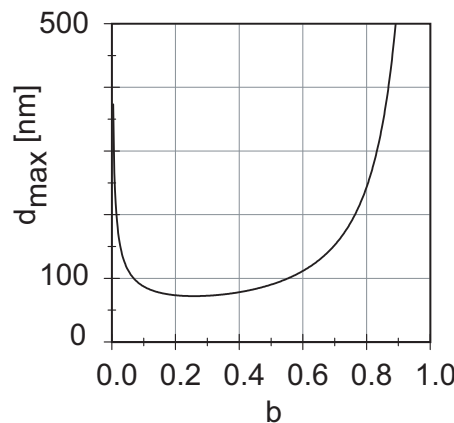


FIG. 6: Dependence of d_{max} , the maximum film thickness for which (tilt) deformations are absent in $a\text{-Mo}_{2.7}\text{Ge}$ -films, on the reduced magnetic field b

It can easily be seen that the relevance of higher order terms goes down with n^{-2} . Together with Eq. 1 we have an expression for the maximum film thickness d_{max} for which deformations of the vortex line by bending are absent. The dependence of d_{max} on b is plotted in Fig. 6 using the parameters for $a\text{-Mo}_{2.7}\text{Ge}$. We find that in the experimental regime of $0.01 < b < 0.3$ for having a 2D system the thickness of the $a\text{-Mo}_{2.7}\text{Ge}$ film should be smaller than ~ 75 nm.

Going back to the data, it appears that at 100 nm the first bending mode becomes relevant, especially for $b > 0.15$. This was not to be expected immediately. For a vortex lattice with strong disorder the length at which the first bending mode appears might actually be much larger, due to the strong renormalization of the elastic constants resulting from the forced disorder. Still, the conclusion is that apparently this consideration is less important, and the scale on which healing starts to appear can be estimated by considering the first bending mode, while, on the other hand, more modes are needed to fully restore the VL.

IV. INTERFACE COUPLING

A. Experimental data

In order to investigate how the interface between NbN and $a\text{-Mo}_{2.7}\text{Ge}$ affects the vortex positions, we prepared a variety of samples with a NbN layer of 67 nm, a 50 nm thick $a\text{-Mo}_{2.7}\text{Ge}$ layer and a ~ 3.5 nm Au layer, where we gradually reduced the interface transparency. Next to a reference sample, we first prepared a sample for which the NbN layer was exposed to pure O_2 gas (~ 18 mbar for 15 minutes) prior to the deposition of the $a\text{-Mo}_{2.7}\text{Ge}/\text{Au}$ layers. The oxidized layer produced in this way is very thin; oxidation in air at temperatures

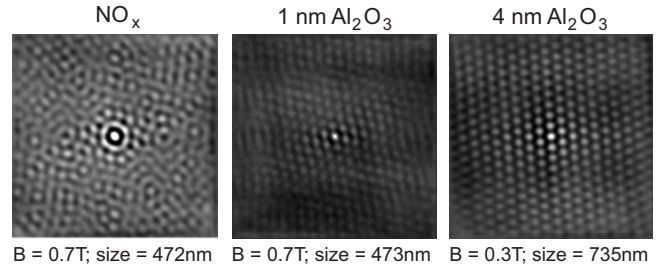


FIG. 7: Autocorrelation maps from vortex lattices measured at 4.2 K on samples with different interfaces. (left) NbN(67)/NbNO/ $a\text{-Mo}_{2.7}\text{Ge}$ (50)/Au, taken at 0.7 T; (middle) NbN(67)/ Al_2O_3 (1)/ $a\text{-Mo}_{2.7}\text{Ge}$ (50)/Au, taken at 0.7 T; (right) NbN(67)/ Al_2O_3 (4)/ $a\text{-Mo}_{2.7}\text{Ge}$ (50)/Au, taken at 0.3 T.

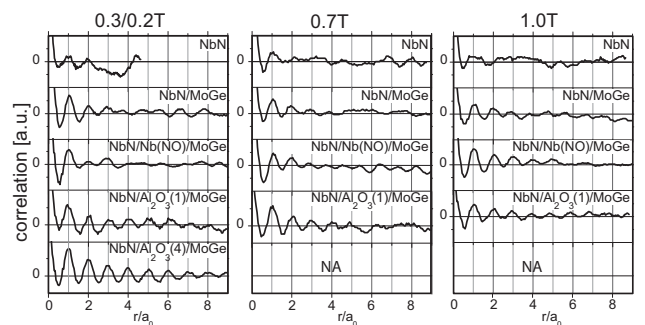


FIG. 8: Comparison of cross-sections from autocorrelation maps of vortex lattices measured at 4.2 K on samples NbN(67)/Au, NbN(67)/ $a\text{-Mo}_{2.7}\text{Ge}$ (50)/Au, NbN(67)/NbNO/ $a\text{-Mo}_{2.7}\text{Ge}$ (50)/Au, NbN(67)/ Al_2O_3 (1)/ $a\text{-Mo}_{2.7}\text{Ge}$ (50)/Au, and NbN(67)/ Al_2O_3 (4)/ $a\text{-Mo}_{2.7}\text{Ge}$ (50)/Au, taken at 0.3 T, at different magnetic fields as indicated. In the left-hand panel, the data on NbN(67)/Au were taken at 0.2 T, all others at 0.3 T.

of 180 °C or less is known to oxidize only the first one or two atomic layers [8]. To reduce the interface transparency even more we deposited an insulating Al_2O_3 interface layer of 1 nm or 4 nm thick in between the NbN layer and the $a\text{-Mo}_{2.7}\text{Ge}$ layer.

In Figs. 7, 8 we present a selection of the acr-images and cross-sections as produced from the raw-data vortex images measured at 4.2 K for various values of B . From the acr-data it can be clearly seen that on changing the interface from 'perfect and thin' to 'insulating and thick' the decoupling of the vortex lattices in the two superconducting layers rapidly sets in, showing already a clear structure for the sample with the oxidized NbN surface. From the cross-sections, for the oxidized surface we find a value for r_c/a_0 of about 4, for the 1 nm Al_2O_3 about 7, and for the 4 nm Al_2O_3 larger than 8 (the maximum for this image size). In other words, the 4 nm insulating interface has completely decoupled the $a\text{-Mo}_{2.7}\text{Ge}$ vortex lattice from the one in the NbN.

B. Shear force versus Josephson coupling

To gain some qualitative understanding for this behavior, we assume that the vortex positions in the template layer are the result of a competition between two forces. One is the Josephson coupling force, which keeps the vortices in the template in registry with those on the other side of the interface. The other is the elastic force which wants to restore the ordered Abrikosov lattice, and which we equate to the shear force necessary to displace a vortex line from its equilibrium position in the lattice. In principle, also the electromagnetic force works to maintain registry, but a simple estimate shows that the electromagnetic coupling is much smaller than the Josephson coupling for the very thin interfaces under consideration. We refer this point to the end of the discussion.

Starting with the shear force, for small displacements $u \ll a_0$ from the ideal lattice positions (the elastic limit) the typical force F_{sh} necessary to move a single vortex line inside the template layer of length d_t over a distance u is given by

$$F_{sh} = c_{66} u d_t = \frac{\Phi_0 B_{c2}(t) u d_t}{16\pi\mu_0\lambda^2} b(1-0.29b)(1-b)^2, \quad (5)$$

where the extrapolation formula of Brandt [9] is used for the elastic modulus c_{66} . This approach does not take into account that the VL may be disordered (not in equilibrium), and may contain defects which soften the lattice, so it should be considered as an upper limit. By rewriting $c_{66} = \Phi_0^2 f(b)/(16\pi\mu_0\lambda^2 a_0^2)$, with $f(b) = (1-0.29b)(1-b)^2$ and using the fact that $b = B/B_{c2} \approx \Phi_0/(a_0^2 B_{c2})$, we can also write F_{sh} in terms of the quantity $\epsilon_0 = \Phi_0^2/(4\pi\mu_0\lambda^2)$ as

$$F_{sh} = \frac{\epsilon_0 u d_t f(b)}{4a_0^2}. \quad (6)$$

For the Josephson coupling force, we start from the expressions for the Josephson energy E_J as function of a displacement of the vortex segment u , given in ref. [10] :

$$\frac{\pi E_J}{\epsilon_0 d_i} = \begin{cases} 0.707 \left(\frac{u}{r_J}\right)^2 \ln\left(\frac{9r_J}{u}\right), & u \leq 2r_J \\ 2.828 \left(\frac{u}{r_J}\right) - 1.414, & 2r_J < u \end{cases} \quad (7)$$

Here, the Josephson length r_J is given by $r_J = \gamma d_i$, with d_i the thickness of the insulating layer and γ the anisotropy parameter of the system defined by $\gamma = \lambda_\perp/\lambda_\parallel = (m_\perp/m_\parallel)^{1/2} = \xi_\parallel/\xi_\perp$. These expressions for E_J are derived from fitting the numerical solutions of a model which consist of two stacks of pancake vortices in an anisotropic superconductor (characterised by its anisotropy parameter γ), displaced with respect to each other by u . For very small displacements, the expression for E_J is equivalent to an earlier one given by Koshelev and Vinokur : $E_J(u) = \frac{\epsilon_0 d_i}{2} \left(\frac{u}{r_J}\right)^2 \ln(r_J/u)$ [11].

For larger displacements, E_J becomes linear in u , which means the Josephson force F_J becomes constant and is simply given by

$$F_J = \frac{2.8 \epsilon_0}{\pi\gamma}. \quad (8)$$

We use this expression as an estimate for the maximum Josephson force [12]. Comparing it to the shear force of Eq. 6, the condition for $F_{sh} \geq F_J$ becomes

$$\frac{u}{a_0} \geq \frac{3.6}{\gamma} \frac{a_0}{dt} \frac{1}{f(b)}. \quad (9)$$

Not surprisingly, the result says that the necessary displacement for the shear force to win from the Josephson coupling force is inversely proportional to the length of the vortex in the template layer (d_t), and also inversely proportional to the anisotropy parameter. For our experiments, typical values are $d_t = 50$ nm and $B = 0.3$ T, which corresponds to $a_0 = 89$ nm and $f(b) \approx 1$, leading to $(u/a_0) \geq 6.4/\gamma$. Assuming a value of $u/a_0 \approx 0.3$ for full disorder, the template layer will become ordered due to shear stress for $\gamma > 20$. This is a very reasonable number for the 4 nm Al_2O_3 interface layer. In a study on multilayers of $a\text{-Mo}_{2.7}\text{Ge}/\text{Ge}$ [13], the following values for (d_i, γ) are quoted : (4.5 nm, 7); (5.5 nm, 13), (6.5 nm, 22). The strong increase with d_i obviously reflects the exponential dependence of the coupling through an insulating interface, and the numbers given above make it quite reasonable to expect that decoupling has not yet been achieved for $\text{Al}_2\text{O}_3(1)$, but occurs for $\text{Al}_2\text{O}_3(4)$. Also, the result indicates that the field dependence of the shear modulus is hardly important in comparison with the dependence on the interface thickness and for given d_i , either coupled or decoupled behavior can be expected for all fields, as is indeed observed.

With the expression for the Josephson coupling force, it is simple to show that the electromagnetic coupling force between two vortex segments can be neglected in our considerations. It was shown by Clem [14] that, for two superconductors characterized by penetration depths $\lambda_{1,2} = \lambda$, with thickness $d_{1,2} = d$ ($d \ll \lambda$), separated by an insulating layer of thickness d_i ($(d_i \ll \lambda)$, the maximum force F_{em} as function of the displacement of the vortex segments with respect to each other is given by

$$F_{em} = \frac{\Phi_0^2}{8\pi\mu_0} \left(\frac{d}{\lambda^2}\right)^2. \quad (10)$$

Here we neglected a weak field dependence which occurs in the regime of interacting vortices, which would lower F_{em} further. Writing Eq. 10 as $F_{em} = \epsilon_0 d^2/(2\lambda^2)$, we find that $F_{em}/F_J = \gamma d^2/(2\lambda^2)$. With d of order 50 nm and λ of order 500 nm for both NbN and $a\text{-Mo}_{2.7}\text{Ge}$, F_{em} is an order of magnitude lower than F_J at the thickness d_i where F_{sh} starts to win from F_J . We should note, however, that this may not be the case for superconductors with smaller values for λ .

V. CONCLUSION

In conclusion, we have used the technique of vortex core imaging by low-temperature STM to study the restoring of initial disorder in a vortex lattice. The disorder was engineered by depositing a weakly pinning superconducting thin film of a -Mo_{2.7}Ge on a strongly pinning layer of NbN. By varying the thickness of the weakly pinning layer, and the interface conditions between both layers, we could reach several conclusions with respect to the healing mechanisms. For clean interfaces we found that the thickness where reordering of the vortex lattice is first observed can be linked to the first bending mode of the vortex lines, without the need to renormalize the elastic constants in the presence of such strong disorder. For our a -Mo_{2.7}Ge layers, this thickness is around 75 nm.

We then used layers with a thickness well below this value in order to investigate the restoration of the vortex lattice when making the interface more insulating. Here we find that the results can be understood in a straightforward way by comparing the Josephson force working to align vortex segments over the interface with the elastic restoring forces inside the weakly pinning layer.

VI. ACKNOWLEDGEMENT

This work is part of the research program of the "Stichting voor Fundamenteel Onderzoek der Materie (FOM)", which is financially supported by NWO. We are grateful to A. E. Koshelev for making us aware of the results of ref. [10].

[1] H. F. Hess, R. B. Robinson, R. C. Dynes, J. M. Valles and J. V. Waszczak, Phys. Rev. Lett. **62**, 214 (1989).

[2] A. M. Troyanovski, J. Aarts and P. H. Kes, Nature **399**, 665 (1999).

[3] Ch. Renner, B. Revaz, K. Kadowaki, I. Maggio-Aprile and Ø. Fischer, Phys. Rev. Lett. **80** 3606 (1998).

[4] Ø. Fischer et al., Rev. Mod. Phys.

[5] G. J. C. v. Baarle, A. M. Troianovsky, T. Nishizaki, P. H. Kes and J. Aarts, Appl. Phys. Lett. **82**, 1081 (2003).

[6] A. Pruyboom, W.H.B. Hoondert, H.W. Zandbergen and P.H. Kes, Jpn. Jn. Appl. Phys. **26**, Suppl. 26-3, 1529 (1987).

[7] r_c is equivalent to the 2D correlation length in the vortex lattice for the overlapping vortex regime ($b > 0.3$; see E. H. Brandt, Phys. Rev. Lett. **57**, 1347 (1986))

[8] R.P. Frankenthal, D.J. Siconolfi, W.R. Sinclair, D.D. Bacon, J. Electrochem. Soc. **130**, 2056 (1983).

[9] E.H. Brandt, Phys. Status Solidi B **77**, 551 (1976).

[10] Y. Y. Goldschmidt and S. Tyagi, Phys. Rev. B **71**, 014503 (2005).

[11] A.E. Koshelev, V.M. Vinokur, Phys. Rev. B **57**, 8026 (1998).

[12] In ref. [10] the case is considered of a kink in a line of pancake vortices, and a correction is proposed to the expression for the Josephson energy in order to take proper account of the fact that the line is not stiff and the kink will be spread over several pancake segments. In our case the line segments are stiff, and the correction would not be appropriate.

[13] W. R. White, A. Kapitulnik and M. R. Beasley, Phys. Rev. B **50**, 6303 (1994).

[14] J. R. Clem, Phys. Rev. B **12**, 1742 (1975).